Drag reduction of a hairy disk

Jun Niu[1,2] and David L. Hu[2,a)]
[1]*College of Engineering, Peking University, Beijing 100871, China*
[2]*Schools of Mechanical Engineering and Biology, Georgia Institute of Technology, Atlanta, Georgia 30318, USA*

(Received 1 June 2011; accepted 25 August 2011; published online 10 October 2011)

We investigate experimentally the hydrodynamics of a hairy disk immersed in a two-dimensional flowing soap film. Drag force is measured as a function of hair length, density, and coating area. An optimum combination of these parameters yields a drag reduction of 17%, which confirms previous numerical predictions (15%). Flow visualization indicates the primary mechanism for drag reduction is the bending, adhesion, and reinforcement of hairs trailing the disk, which reduces wake width and traps "dead water." Thus, the use of hairy coatings can substantially reduce an object's drag while negligibly increasing its weight. © *2011 American Institute of Physics*. [doi:10.1063/1.3639133]

Scales, hair, and feathers have been classically known for their insulative and protective functions.[1] Recently, they have attracted much attention for their role in passive flow control, as they can self-adapt to direct flows without the input of energy.[2–4] This makes them fundamentally different from man-made flow control systems. However, due to the difficulty in monitoring high-speed animal movements and quantifying the properties of the complex surface structures themselves, passive flow control mechanisms in biology remain poorly understood.

Flow-controlling surfaces have a wide diversity in the animal kingdom. They have evolved to reduce an animal's induced drag, which in turn increases its speed and saves energy. A great variety of passive flow control mechanisms are used by birds. Wing tip feathers form slots that reduce drag by spreading vorticity horizontally along the wings.[5] Tail feathers reduce drag by acting as a combined wedge and splitter plate to control vortex shedding and body wake development.[6,7] Many birds will also pop-up their wing feathers upon landing, a behavior which is hypothesized to control lift fluctuations.[3] Despite these numerous biological examples, little attention has been paid to understanding the mechanisms by which long flexible filaments can affect flow.

Our study is inspired by Favier *et al.*,[8] who recently developed a two-dimensional numerical method for simulating a feather system mimicking that of birds.[8] Their study was limited to feathers consisting of short rigid hairs hinged at the base and at Reynolds numbers of 200, far less than that of flying birds. Nevertheless, they show that coating a disk with hairs can reduce drag by 15% and lift fluctuation by 40% relative to a bald disk. In our study, we test their numerical prediction using direct force measurement and flow visualization of a hairy disk.

To mimic an animal's furry coat, we affix soft rubber threads (diameter $d = 0.25$ mm, mass density $\rho_{hair} = 985.73$ kg/m^3, and bending modulus $EI = 3.4 \times 10^{-10}$ N·m^2) along the downstream edge of a Styrofoam disk (diameter $D = 16.5$ mm), as shown in Fig. 1(a). Hairs are coated symmetrically on the disk, where L denotes the length of each hair, b the hair center-to-center spacing, and α the angle between the root of the outermost hair and the stagnation streamline.

In our experiments, the number of hairs m on each disk varies from two to ten. We define a 2-D hair density $\phi = md/[(m-1)b + d]$ as the ratio of the hair profile area to the total area coated by hairs. We derive a simple conversion from our 2-D hair density ϕ to an equivalent 3-D hair density ϕ_{3D}, which we use in Fig. 2 to compare our experiments to previous numerical results.[8] If hairs on the 3-D cylinder in Favier *et al.*[8] are uniformly distributed at a center-to-center distance b as shown in Fig. 1(b), the 3-D hair density can be approximated as $\phi_{3D} \approx \pi d^2/4b^2$. Moreover, in the limit of large number of hairs m, the 2-D hair density scales as $\phi \approx d/b$. Consequently, these two densities satisfy the relation $\phi_{3D} \approx \pi\phi^2/4$. We note that this relation becomes less accurate as hair densities approach zero.

The experimental setup is shown in Fig. 1(c). A soap film water tunnel generates an approximately 2-D flow[9,10] around our hairy disk. The soap solution (density $\rho = 998.2$ kg/m^3 and viscosity $\mu = 0.00399$ Pa·s) is made by adding 1% detergent to water.[9] After falling from an overhead reservoir, the solution is stretched between two parallel nylon threads of separation 107 mm. The width of the film is much larger than the disk diameter, making boundary effects of the water tunnel negligible. The soap flow rate is fixed at 50 ml/min, corresponding to a free-flow velocity $U = 1.947$ m/s, as measured by tracer particles. The Reynolds number based on the disk diameter is $Re = \rho UD/\mu \approx 8 \times 10^3$, which is within the range of typical Reynolds number for flying birds.[11] At this Reynolds number, we observe the free stream is laminar and the wake of the disk is turbulent. The film's fragility at larger sizes and slower speeds limits our choices of Reynolds number, disk, and hair sizes: a low $Re \approx 200$, as in Favier *et al.*[8] is not feasible since such slow flow renders the soap film fragile.

An important dimensionless number used in our study is the Cauchy number, the ratio of the fluid kinetic energy to the elastic energy of a single hair or hair clump.[12,13] In these cases, the Cauchy number may be written as $C_Y = \frac{\rho U^2 L^3 \xi}{16(EI)^*}$,

a)Author to whom correspondence should be addressed. Electronic mail: hu@me.gatech.edu.

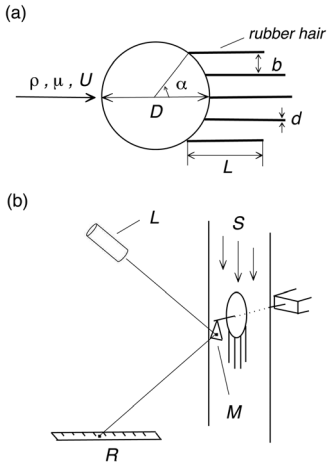

FIG. 1. (a) Schematic of the hairy disk in our experiment;[8] (b) Our optical method for measuring the drag force exerted on a hairy disk (adapted from Alben *et al.*[10]). Here, S denotes the soap film, M a small mirror, L a laser beam and R a ruler.

where the effective bending modulus of a single hair is $(EI)^* = EI$ and the hairs are immersed in a soap film of thickness $\xi \approx 4\ \mu$m (Ref. 9) much less than a hair diameter. In our experiments, we increase hair length L from $D/4$ to $2D$, providing a range of C_Y from 0.2 to 100 from which we expect hair flapping to occur if $C_Y > 1$.

We apply the optical method of Alben *et al.*[10] to measure the induced drag force F_D exerted on the disk as shown in Fig. 1(c). In our experiments, we observed that the drag force was periodic; we present here the average drag over a period. The dimensionless drag coefficient C_D is defined as $C_D = F_D/(\frac{1}{2}\rho U^2 A)$ where A is the characteristic frontal area of the disk, here, a constant $\xi D = 6.8 \times 10^{-8}$ m^2. To highlight the hydrodynamic benefits of the hairs, we define a relative drag coefficient C_r as the drag coefficient of the hairy disk $C_{D,hairy}$ divided by the drag coefficient of a bald disk of the same diameter, $C_{D,smooth}$. Our experiments yield $C_{D,smooth} = 1.1$, which is in close agreement with the drag coefficient of a cylinder in a 2-D flow under the same Reynolds number;[14] this agreement validates the accuracy of our experimental methods. In a series of experiments, we investigate the influence of hair density ϕ, coating area α, and relative hair length L/D on the disk's drag force. For each data point plotted in Figs. 2–5, we constructed a new disk according to the geometry and spacing of the hairs specified. We measured drag using at least five trials with each disk. Error bars indicate the standard deviation of measurement.

In Fig. 2, we report the change in relative drag coefficient C_r with hair density ϕ. The relative hair length L/D and coating angle α are fixed at 0.5 and 47°, respectively. A disk with two hairs ($\phi = 0.041$) increases drag by 15% relative to a bald disk, whereas disks with hair densities of $\phi > 0.081$ enjoy a slight drag reduction (5%-10%). Flow visualizations indicate the primary reason for drag increase is the flapping of the hairs. The onset of flapping in flags and filaments has been shown to increase drag.[9,15,16] When hair density is low (e.g., on a disk with 2-3 hairs), drag is increased because each hair has sufficient space to flap. Conversely, when hair

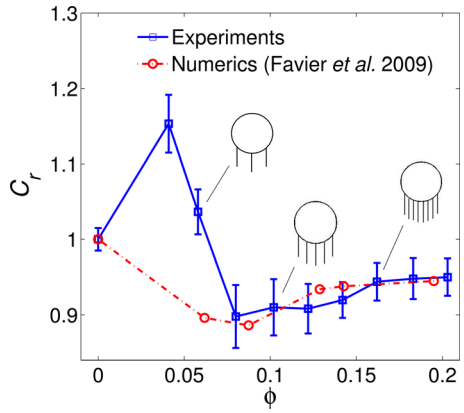

FIG. 2. (Color online) Variation of the relative drag coefficient with hair density. Dimensionless hair length and coating angle are fixed as 0.5 and 47°, respectively. Measurement of each data point is repeated several times and the error bars represent the standard deviation of the measurements.

density is high, drag remains unchanged because the hairs' close proximity suppresses flapping. Later, we present reasons for the drag reduction observed.

As shown by the dashed line in Fig. 2, our experimental results compare favorably with previous numerical predictions,[8] despite the different conditions used by Favier *et al.* (hair lengths $L = 0.2\ D$, coating angles $\alpha = 72°$, and Reynolds number $Re = 200$). We note Favier *et al.* neglected to observe the global peak in drag at $\phi = 0.041$, but we suspect they would have found such results had their model accounted for fluttering.

Figure 3(a) shows the relation between relative drag coefficient C_r and coating angle α, with the numerical result[8] plotted for comparison. In our experiments, relative hair length and density are fixed at 0.5 and 0.105, whereas in the numerics, values of 0.2 and 0.0874 are used. Despite different regimes of hair length, density, and Reynolds number, both numerics and experiments make clear the advantage of enlarging the disk's coating area until the coating angle reaches a critical value α^*. In our case, α^* is approximately

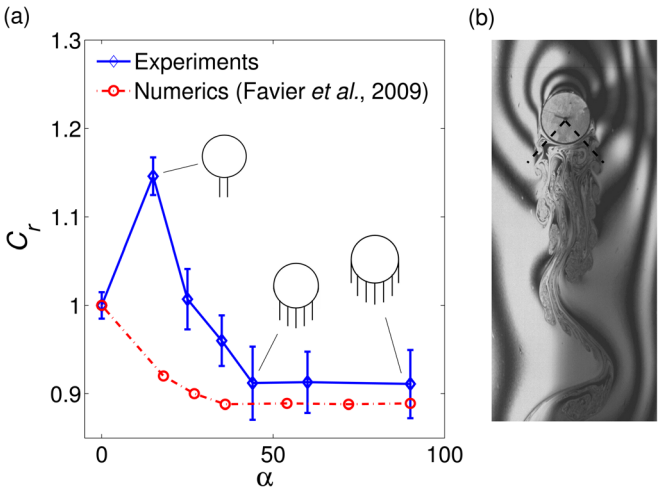

FIG. 3. (Color online) (a) Variation of the relative drag coefficient with coating area. Dimensionless hair length and hair density are fixed as 0.5 and 0.105, respectively. (b) Flow visualization of a bald disk, with the boundaries of its recirculation region denoted by dashed lines.

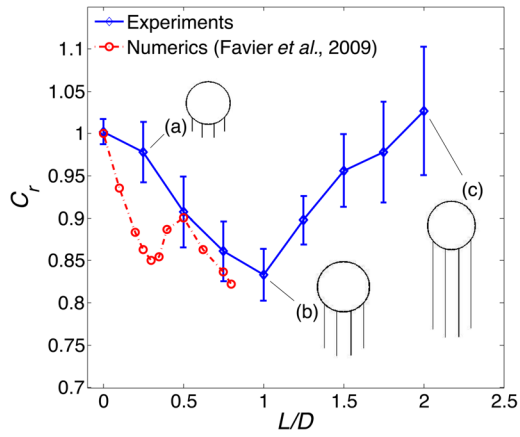

FIG. 4. (Color online) Variation of the relative drag coefficient with dimensionless hair length. The hair density and coating angle are fixed as 0.081 and 47°, respectively.

42° which is slightly larger than that of the numerics (36°) in part because of the higher Reynolds number in our experiments. These values are comparable to the limited area of recirculation behind a bald disk, shown occupying approximately a quarter of the disk perimeter in Fig. 3(b). The addition of hairs at coating angles between 42° to 90° has little effect on the drag force. We conclude that for reducing drag, hairy coatings are only needed in the downstream region, as is consistent with the results of Favier *et al*. Disks with coating angles $\gg \alpha^*$ (e.g., a disk covered in hair) will suffer an increase in drag due to their larger frontal surface areas.

Based on our findings on optimal hair density and coating area, we choose the optima $\alpha = 47°$ and $\phi = 0.081$ (corresponding to a four-hair disk) to investigate the effects of hair length in the following series of experiments. Fig. 4 shows the drag force for relative hair lengths between 0 and 2. Most strikingly, at an optimal hair length $L/D \approx 1$, drag is reduced by 17%, a value nearly identical to that predicted by Favier *et al*. (15%). The authors' results for long hairs ($L/D = 0.6$-0.8) are beyond the regime of validity of their model, which is based on rigid hairs attached by flexible hinges and so cannot account for hair bending; nevertheless, their model seems to capture the trends near $L/D = 1$ well. The presence of the

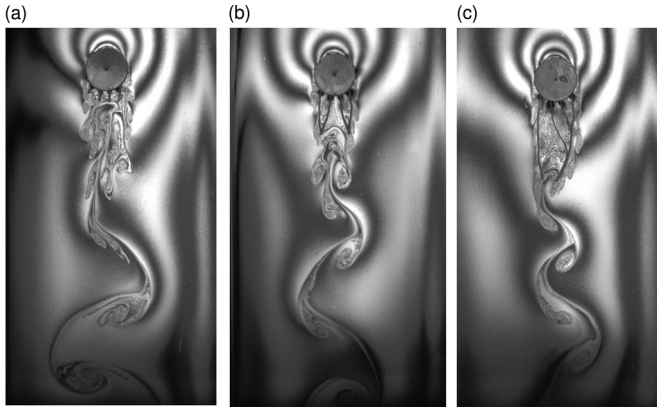

FIG. 5. Visualization of the flow around a hairy disk with relative hair lengths $L/D = 0.25$, 1, and 2, corresponding to the three points labelled in Fig. 4. Hair density and coating angle are fixed as 0.081 and 47°, respectively (enhanced online) [URL: http://dx.doi.org/10.1063/1.3639133.1].

local minimum at $L/D = 0.3$ from Favier *et al*. was not repeatable in our experiments, but we speculate that the flexible hinges at the base of their hairs may have produced such results. In contrast, our hairs were rigidly attached to the disk, in analogy with natural hair and feathers.

Using flow visualization, we find that drag is reduced primarily because of the trapping of "dead water" by the hairs. Dead or stagnant water reduces drag because it increases pressure at the downstream end of bodies,[17] thus equalizing up and downstream pressure. Flow visualization[25] of the three disks with hair lengths $L/D = (0.25, 1, 2)$ is shown in Figs. 5(a)–5(c), corresponding to the three points (*a*–*c*) in Fig. 4. Fluid in the dead water region (spanning 0.1 to 2 disk diameters behind the disk) is nearly static (about 1 mm/s), and two orders of magnitude slower than the recirculating flow in the same position behind a bald disk (Fig. 3(a)). Elongation of the dead water region by longer hairs further decreases drag,[8] as seen in Figs. 5(a)–5(b) and the reduction in drag in Fig. 4. However hairs that are longer than $L/D = 1$ increase drag, as shown in Fig. 5(c). Below, we rationalize this variation in drag according to the clumping of hairs.

The rubber hairs used in our experiments experience negligible adhesion if dry. Their rough surfaces prevent asperities on the hairs from contacting, weakening van der Waals attraction.[18] However, we can increase inter-hair adhesion by embedding the hairs in a soap film. Rubber hairs are wetting with soapy water and thus, they generate lateral capillary attraction, which decays exponentially with hair spacing.[19,20] At the optimum hair length ($L/D = 1$), this attractive force is sufficient to adhere pairs of hairs together at their tips, resulting in the hair clumps shown in Fig. 5(b). This hair clump has advantageous properties. Namely, it has a smaller C_Y, associated with greater rigidity with respect to fluid drag and less vibration. These hair clumps guide flow streamlines around them, encouraging the recombination of separated flow, and controlling wake width according to their distance of separation. The reduction in drag via control of wake width has also been shown to be important in avian flight. By comparing the wakes of frozen birds with clipped and unclipped tailfeathers, Maybury and Rayner (2001) showed intact tail feathers benefit birds by generating a smaller wake width and a lower drag.[7] Thus, the hairs in Fig. 5(b) can be viewed phenomenologically as self-assembling 2-D tail feathers, adjoined by surface tension. In both systems, adhesion may be a necessary mechanism for stiffening hairs. In birds, inter-feather adhesion is accomplished in the form of frictional interactions between hooklets on barbules.[21]

If hairs are longer than $L/D = 1$, they adhere together in a random fashion, and can no longer stably stiffen each other, as shown in Fig. 5(c) and Supplementary Video 3 (Ref. 25). Although these hairs indeed trap dead water, the net drag reduction is offset by the long hair length which causes sufficient vibration that drag is increased by 3%. These hairs resemble long flags trailing behind the disk which clearly accrue drag.

As hairs shorten from $L/D = 1$, their influence on the drag of the disk diminishes. Figure 5(a) shows the shortest hairs we studied, with lengths $L/D = 1/4$. The rigidity of the

hairs impede bending, allowing them to remain straight at the flow speeds studied. The straightness of the hairs causes drag to be nearly the same (±4%) as that of a bald disk. This result is consistent with our previously hypothesized mechanism for drag reduction. First, since the hairs do not coalesce, the disk's wake is 20% wider than in Fig. 5(b), indicating that short hairs ($L/D = 1/4$) cannot control wake width. Secondly, less dead water is trapped than in Fig. 5(b), reducing the dead water to an amount that has a negligible influence on drag.

If hairs are sufficiently short, their vibration may in fact help reduce drag. Favier *et al.*[8] proposes a mechanism of drag reduction via the synchronization of vortex shedding with vibrating hairs. By tracking the vibration of short hairs ($L/D < 3/4$) in our experiments, we find support for this hypothesis. First, we observe a striking correspondence between hair vibration and vortex shedding frequencies. For a disk with 4 hairs of length $L/D = 1/2$, the vibrating frequency of the two innermost hairs $f_h = 26.2 \pm 1.2$ Hz is within 2% of the vortex shedding frequency $f = 26.7 \pm 1.0$ Hz (in $N = 10$ trials on a single disk). The correspondence between f and f_h is further highlighted by their substantial dissimilarity to the hair's natural frequencies (116 Hz), as predicted from relations based on the fluid properties and hair geometry.[22,23] Second, we find the dimensionless vortex shedding frequency $St = fD/U = 0.226$ for the same hairy disk is 6% less than that for a bald disk ($St = 0.240$ as we measured). We validate our St value for bald disks with those experimentally measured and numerically predicted ($St = 0.237$) for a 2-D cylinder at Reynolds numbers of 1000.[24] A statistical t-test at the 5% significance level confirms the dimensionless vortex shedding frequency of the hairy disk is different from that of the bald disk. In sum, our observations are at least consistent with the hypothesis of drag reduction via synchronization of the hairs to the vibrating wake.

In conclusion, we have investigated the hydrodynamic benefits of coating a disk with hair. Our study demonstrates that hairy coatings, with carefully chosen spacings, lengths, and coatings areas, can substantially reduce an object's drag while negligibly increasing its weight. According to our work and that of Favier *et al.*, drag can be reduced by 17% at both high and low Reynolds numbers (10^4 and 10^2). Our work highlights the importance of interactions between hairs, which was not examined closely in Favier's work. We show that the greatest drag reduction occurs when hairs are sufficiently long and spaced sufficiently closely that capillary attractive forces can adhere them together. These reinforced hairs resist vibration, trap dead water, reduce the wake width of the disk, all of which act together to reduce a disk's drag.

Hairy surfaces may also reduce lift fluctuations. Favier *et al.*[8] reported lift coefficients are reduced by 40% using hairy coatings. Our qualitative measurements also suggest a hairy coating reduces the amplitude of lift fluctuations.

Our study focused on the effects of changes in hair spacing and length rather than hair stiffness. Feathers are known to have heterogeneous stiffness, with stiff rachides and flexible barbules. A detailed examination into the optimal levels of adhesion and stiffness would yield further insight into the design of passive flow control in hairy and feathery systems.

J. Niu acknowledges the support of the China Scholarship Council and D. Hu the support of the NSF (Grant PD08-7246).

[1]V. Sokolov, *Mammal skin* (University of California Press, Berkeley, CA, 1982).
[2]F. Fish and G. Lauder, "Passive and active flow control by swimming fishes and mammals," Annu. Rev. Fluid Mech. **38**, 193 (2006).
[3]W. Liebe, "Der Auftrieb am Tragflugel: Entstehung und Zusammenbruch," Aerokurier **12**, 1520 (1979).
[4]E. van Nierop, S. Alben, and M. Brenner, "How bumps on whale flippers delay stall: An aerodynamic model," Phys. Rev. Lett. **100**, 54502 (2008).
[5]V. Tucker, "Drag reduction by wing tip slots in a gliding Harris' hawk, Parabuteo unicinctus," J. Exp. Biol. **198**, 775 (1995). Available at http://jeb.biologists.org/content/198/3/775.abstract?sid=d007f7a1-8abb-4a16-b873-1fd717f72866.
[6]A. Thomas, "Why do birds have tails? The tail as a drag reducing flap, and trim control," J. Theor. Biol. **183**, 247 (1996).
[7]W. Maybury and J. Rayner, "The avian tail reduces body parasite drag by controlling flow separation and vortex shedding," Proc. R. Soc. London, Ser. B **268**, 1405 (2001).
[8]J. Favier, A. Dauptain, D. Basso, and A. Bottaro, "Passive separation control using a self-adaptive hairy coating," J. Fluid Mech. **627**, 451 (2009).
[9]J. Zhang, S. Childress, A. Libchaber, and M. Shelley, "Flexible filaments in a flowing soap film as a model for one-dimensional flags in a two-dimensional wind," Nature **408**, 835 (2000).
[10]S. Alben, M. Shelley, and J. Zhang, "Drag reduction through self-similar bending of a flexible body," Nature **420**, 479 (2002).
[11]M. Denny, *Air and Water: The Biology and Physics of Life's Media* (Princeton University Press, Princeton, NJ, 1993).
[12]E. de Langre, "Effects of wind on plants," Annu. Rev. Fluid Mech. **40**, 141 (2008).
[13]F. Gosselin and E. de Langre, "Drag reduction by reconfiguration of a poroelastic system," J. Fluids Struct. (to be published).
[14]H. Schlichting, *Boundary Layer Theory* (McGraw-Hill, New York, 1979).
[15]M. Shelley and J. Zhang, "Flapping and bending bodies interacting with fluid flows," Annu. Rev. Fluid Mech. **43**, 449 (2011).
[16]S. Taneda, "Waving motions of flags," J. Phys. Soc. Jpn. **24**, 392 (1968).
[17]M. Pastoor, L. Henning, B. Noack, R. King, and G. Tadmor, "Feedback shear layer control for bluff body drag reduction," J. Fluid Mech. **608**, 161 (2008).
[18]D. Tabor, "Surface forces and surface interactions," J. Colloid Interface Sci. **58**, 2 (1977).
[19]P. Kralchevsky and N. Denkov, "Capillary forces and structuring in layers of colloid particles," Curr. Opin. Colloid Interface Sci. **6**, 383 (2001).
[20]D. Hu and J. Bush, "Meniscus-climbing insects," Nature **437**, 733 (2005).
[21]J. Dyck, "The evolution of feathers," Zool. Scr. **14**, 137 (1985).
[22]C. Van Eysden and J. Sader, "Resonant frequencies of a rectangular cantilever beam immersed in a fluid," J. Appl. Phys. **100**, 114916 (2006).
[23]L. Landau and E. Lifshitz, *Theory of Elasticity*, 3rd ed. (Pergamon Press, Oxford, 1986).
[24]C. Wen and C. Lin, "Two-dimensional vortex shedding of a circular cylinder," Phys. Fluids **13**, 557 (2001).
[25]See supplementary material at http://dx.doi.org/10.1063/1.3639133 for video showing the hair vibration in the soap flow with dimensionless hair length $L/D = 0.5$. Time is slowed 35X.